INTERNATIONAL JOURNAL OF STRUCTURAL CHANGES IN SOLIDS – Mechanics and Applications
Volume 3, Number 1, February 2011, pp.1-13

IJSCS

The Bauschinger Effect in Different Heat Treatment Conditions of 42CrMo4

A. Ellermann * and B. Scholtes
University of Kassel, Institute of Materials Engineering, Mönchebergstraße 3, 34125 Kassel, Germany

Abstract

Although the Bauschinger effect was investigated for many materials, there are only few results concerning hardened or low annealed steels. Since those materials often are plastically deformed, e.g. due to straightening processes, there is a great concern to know about the effect of the material on the Bauschinger effect and its relation to changes in microstructure. Hereby uncertainties in daily application of work pieces can be avoided and straightening processes may be improved. The Bauschinger effect is examined in the steel 42CrMo4 in common heat treatment conditions in tension-compression as well as in bending tests with load reversal. In addition X-ray examination is carried out to measure the development of residual stresses in the material. In particular it is shown that there is no direct correlation between the strength of the material and the magnitude of the occurring Bauschinger effect.

Keywords

Bauschinger effect; martensite; bainite; ferrite; pearlite; annealed; plastic deformation, tension-compression; 4-point bending; residual stress; strength differential effect; pre-strain

1. Introduction

Many manufacturing operations like joining or heat treatment are associated with the occurrence of distortion [Heeß 2003, Klein et al. 2005]. It is well known that distortion is linked in a complex way to the parameters of manufacturing throughout the whole manufacturing chain which impedes total elimination of distortion. That is why the correction of distortion (straightening) becomes mandatory to make a work piece fulfil the demands concerning geometry and accuracy.

From the point of view of a materials scientist, straightening processes are well defined plastic deformations that affect the microstructure of the material. This means a change of dislocation densities and arrangements but it is also possible that deformation twins or phase transformation occur. Depending on the straightening process, changes in microstructure can be both homogenous and inhomogeneous within the cross section of the work piece. As a consequence, straightening processes are associated with a change in the strength of the materials. Depending on the direction of subsequent loading, the material's yield strength may increase (hardening) or decrease (softening). In the latter case the Bauschinger effect plays an important role, since it can lead to a drastic loss of strength. When plastic deformations are micro- or macroscopically inhomogeneous, existing residual stresses may be relocated and new residual stress distributions can be observed. Finally load-induced phase transformations can occur which has to be taken into account for the behaviour of a work piece.

Although the Bauschinger effect has been researched systematically for many metallic materials in different heat treatment conditions, there still is only little information concerning hardened or low annealed steels. Since these conditions often feature plastic deformation that is caused by the manufacturing process, e.g. straightening, there is a great concern about understanding the consequences of the Bauschinger effect in those cases and its dependency of the microstructure originating from heat treatment. Thus, uncertainties in daily application may be deleted and strategies for straightening processes may be deduced.

The current project deals with the Bauschinger effect of the two steels 42CrMo4 and C45E in differently heat treated conditions with the aim to analyse the microstructure, its properties and the resulting Bauschinger effect. Therefore, tension-compression tests as well as bending tests with load reversal were conducted. In addition, X-ray examinations are used for determination of macro- and micro residual stresses in the material.

In 1886, Johann Bauschinger discovered the phenomenon that the yield strength of steels previously deformed above the (tensile or compressive) elastic limit, tends to zero when loaded in the reverse direction [Bauschinger 1886]. This effect was named after Bauschinger. Until now, the cause of the Bauschinger effect has not been clarified in detail, but it is assumed that it is strongly related to residual stresses and mobile dislocations in the material [Li et al. 1978, Scholtes 1980]. In earlier theory, the Bauschinger effect was related to internal stress effects and especially the microscopic residual stress development as a result of inhomogeneous deformation of the grains [Abel et al. 1972].

*Corresponding author: email: a.ellermann@uni-kassel.de, Tel. +49 561 804 3701

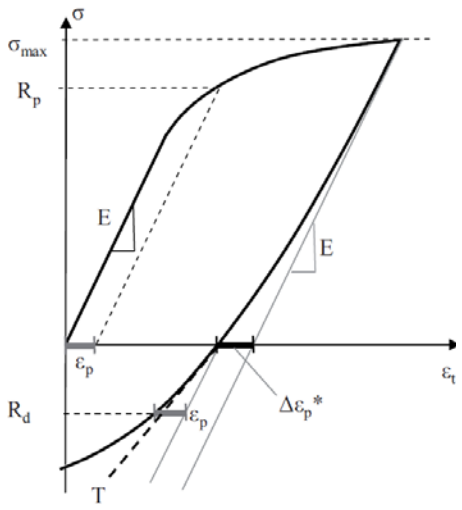

Figure 1 Schematic drawing of Bauschinger parameters

Other investigations were based on the dislocation theory that made back-stresses and dislocation pile-ups responsible for the Bauschinger effect [Abel et al. 1972]. Nowadays one can assume that the Bauschinger effect is related to the direction of loading and anisotropic behaviour in the resistance to dislocation movement. These movements mean plastic deformation on both macro and micro scale which also influence the residual stress state in the microstructure.
By now, various investigations concerning the Bauschinger effect in different materials like in copper [Scholtes et al. 1986, Gokyo et al. 1970, Wooley 1953], nickel [Woolley 1953], aluminium [Wooley 1953], magnesium [Noster et al. 2003] and different kinds of steels [Scholtes at al. 1986, Scholtes et al. 1985, Scholtes 1980, Scholtes et al. 1983, Ring et al. 1993, Woolley 1953] were carried out.

Since it is not possible to describe the characteristics of the Bauschinger effect using a single parameter, various adequate parameters shall be discussed, that show how the Bauschinger effect affects the material's properties. Figure 1 shows the characteristic change in the deformation behaviour when the material is deformed plastically and thereafter loaded in reverse direction. After loading to σ_{max}, one can observe a non-linear unloading curve. The following curve at reversed load does not show a real yield stress anymore which means that even small loads in reverse direction cause immediate plastic deformation. The parameters used are the plastic back-deformation $\Delta\varepsilon_p^*$ and the proof stresses R_p in tension as well as R_d in compression. The tangent modulus T characterizes the hardening behaviour of the stress-strain curve after load reversal.

Hoff and Fischer [Hoff et al. 1958] reported that the Bauschinger effect in copper increases rapidly with increasing tensile stress. In plastically deformed material, the Bauschinger effect was not isotropic for all directions. In addition, it was found that hardness does not seem to be a direct indicator for the change in the deformation behaviour when the material is deformed plastically. Due to prior research, there already exists information concerning the Bauschinger effect in heat treated steels, especially in normalized steels. Scholtes [Scholtes et al. 1986, Scholtes et al. 1985, Scholtes 1980] found the interrelation that the Bauschinger effect increases with an increasing content of cementite/ pearlite and an increasing fineness of cementite lamellas in pearlite. Studies on copper and Brass in [Gokyo et al. 1970] report that the Bauschinger effect is directly controlled by the number of piled-up dislocations caused by strain hardening. However, the few results of examinations dealing with the Bauschinger effect in hardened and annealed steels are contradictory in part.

2. Materials and Experimental Details

2.1 Heat Treatment and Microstructures

The examination was done on differently heat treatment conditions of the steel 42CrMo4 (1.7225, AISI 4140QT, chemical composition: 0.42wt% C; 1.02wt% Cr; 0.17wt% Mo). Table 1 shows the parameters of the heat treatment and the resulting hardness of the material.

Table 1 Heat treatment conditions of 42CrMo4

Cond.	Hardening	Annealing	Microstructure	Hardness, HRC
E	850°C 20min / oil 80°C	240°C 60min	annealed martensite	52
F	850°C 20min / oil 80°C	350°C 60min	annealed martensite	48
G	850°C 20min / 360°C 240min	--	bainite	36
H	850°C 20min / air	--	ferrite/ pearlite	30

Table 2 Heat treatment conditions of C45E

Cond.	Austenitisation	Annealing	Microstructure	Hardness, HV10
N	880°C 60min / furnance	--	ferrite/ pearlite	140

In addition, a normalized steel C45E (1.1191, SAE1045, chemical composition; 0.44wt% C) was examined as well to compare the results, since the material was the object of many prior investigations like [Scholtes et al. 1986, Scholtes et al. 1985, Scholtes 1980]. The parameters of heat treatment are shown in Table 2.

The microstructures of 42CrMo4 resulting from the heat treatment are shown in Figure 2. Condition E and F show a typical annealed microstructure that consists of lower bainite, pro-eutectoid precipitated ferrite and very fine martensite. In the micrograph of E one can detect chromium carbides as well. Condition G mainly consists of lower bainite and proeutectoid precipitated ferrite. Condition H can be considered as normalized and consists of ferrite/ pearlite and a little amount of bainite.

Figure 3shows the microstructure of the normalized C45E. Although the magnification is somewhat lower one can clearly see the ferrite and pearlite grains.

Figure 4 shows the results of tensile tests for each heat treatment condition. According to DIN 50125, the tests were carried out on cylindrical specimens with a diameter of 7mm and a gauge length of 40mm.

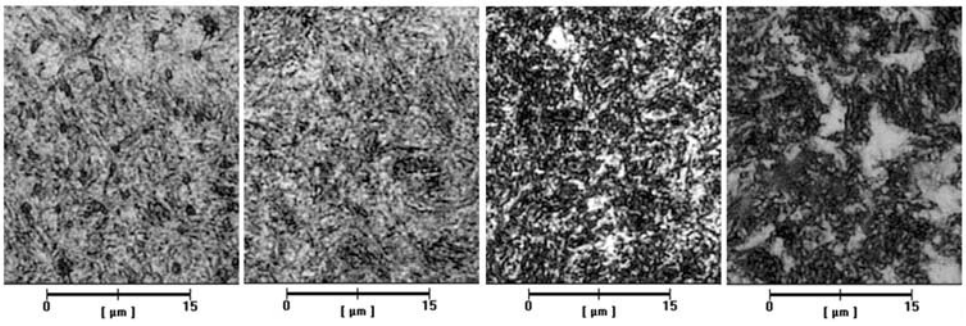

Condition E Condition F Condition G Condition H

Figure 2 Microstructure of the heat treatment conditions of 42CrMo4.

Condition N

Figure 3 Microstructure of the normalized C45E

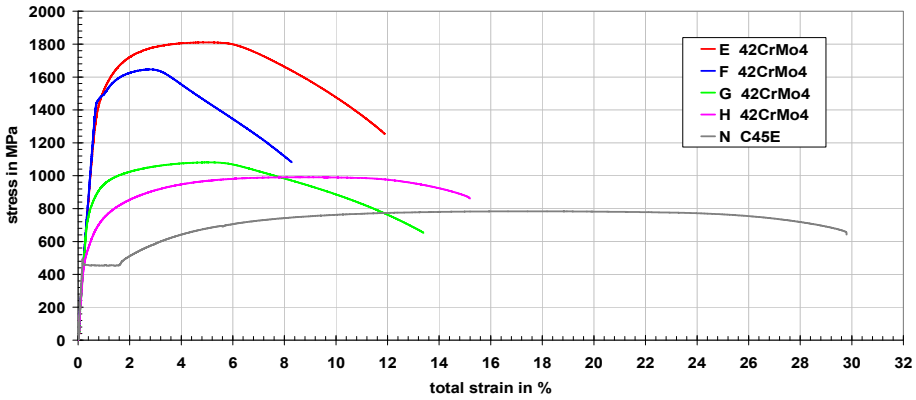

Figure 4 Tensile tests of conditions of 42CrMo4 and C45E

The low annealed martensite condition E shows a high yield stress followed by work-hardening. The annealed martensite condition F almost has a similar yield strength, but a lower ultimate tensile stress and a smaller fracture strain. The bainite condition G shows a yield stress that is only half of the martensite conditions E and F. The normalized condition H is similar to the bainite one, but somewhat lower in yield- and ultimate tensile stress. The normalized C45E, condition N, shows the lowest yield stress, a distinctive Lüders strain and almost the double elongation at fracture than the other 42CrMo4 conditions. Both the soft conditions H and N only show a small contraction at breaking point. The mechanical properties of the steels investigated are listed in Table 3.

Table 3 Materials' properties

Condition	E in GPa	$R_{p0,2}$ in MPa	R_m in MPa	A in %
E	202	1510	1820	10.6
F	203	1480	1640	8.1
G	207	850	1080	13.2
H	206	590	980	14.2
N	212	350	600	28.0

2.2 Specimens and Mechanical Tests

The specimen shown in Figure 5 was designed to fulfil several requirements of a tension-compression test. On the one hand, it was necessary to design a short specimen to prevent buckling at compressive load; on the other hand the specimen had to be long enough to be mountable in the fixtures. The chosen geometry enabled form-locking clamping for adequate loading in tension and compression. The specimens were heat treated in an oversize shape to prevent surface decarburization and to correct possible distortion. Later on the specimens were hard turned to the geometry of Figure 5.

According to the demands and the dimensions of the applied 4-point bending device, the geometry of the bending specimen is shown in Figure 6. It is a massive rectangular rod. Since the deflection of the bending device was limited, the specimens were designed with an increased bending height of 15mm. The bending test specimens were heat treated in oversize to prevent surface decarburization and to correct possible distortion. Later, the specimens were ground to the geometry of Figure 6.

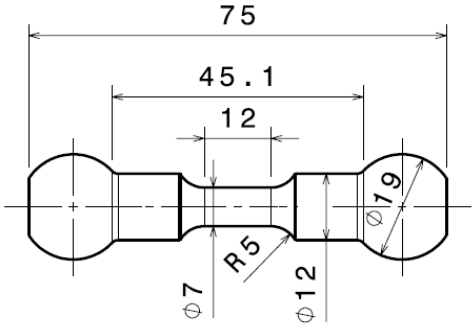

Figure 5 Geometry of tension-compression test specimens

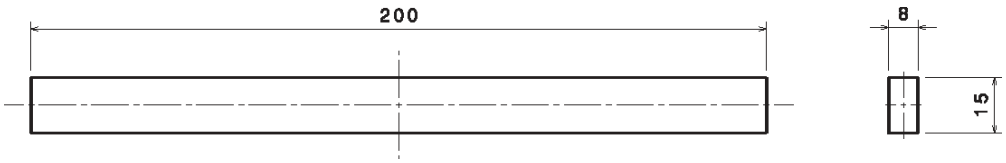

Figure 6 Geometry of bending test specimens

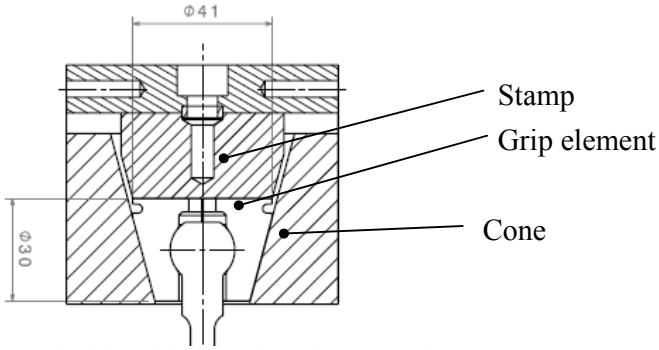

Figure 7 Cross sectional view of the fixture for tension-compression tests.

The tension-compression tests were carried out on an electro mechanical "Zwick Z100" tensile testing machine with hydraulic wedge fixtures. Since the specimens shown in Figure 5 required a special fixture, a new clamping system was developed, see Figure 7. The ball head of the specimen is clamped by four grip elements that are hydraulically pressed in the cone of the chuck. This system enabled clamping the hard specimens by form-locking and minimized bending due to clamping. On the cylindrical body of the specimen, slim strain gauges were attached in longitudinal direction and wired as quarter Wheatstone bridges. The tests were carried out with a constant cross head speed of 0.2mm/ min at loading and unloading.

The bending tests were carried out on a 4-point bending test device (see Figure 8), mounted on a 200kN electro mechanical tensile testing machine "Zwick 1484". The device consists of two pairs of rolls with 15mm in diameter. In order to reduce friction, the rolls were mounted pivotally in needle roller bearings. According to DIN EN 685-3, the distance of the upper rolls was 70mm, of the lower ones 140mm. Two strain gauges were attached in the centre area on the top side as well as on the bottom side of the specimen to measure the strain in the outer fibre of the bending specimen. By using the relation

$$\sigma_R^* = M_b / W_b$$

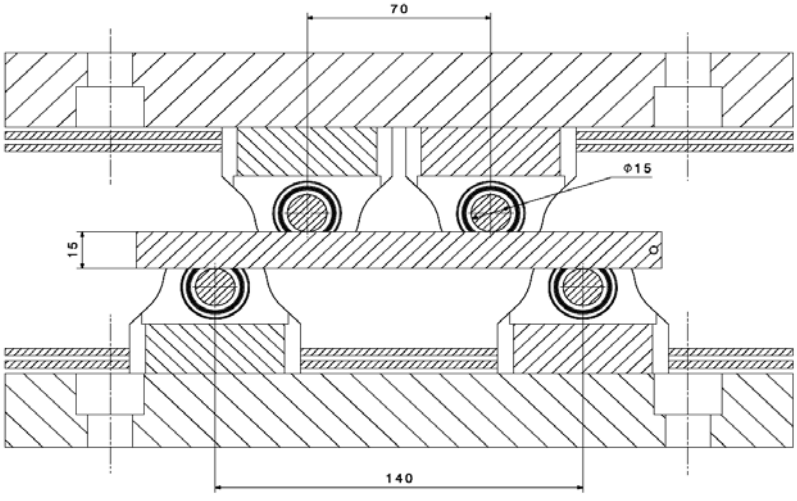

Figure 8: Cross sectional view of the 4-point bending device with specimen

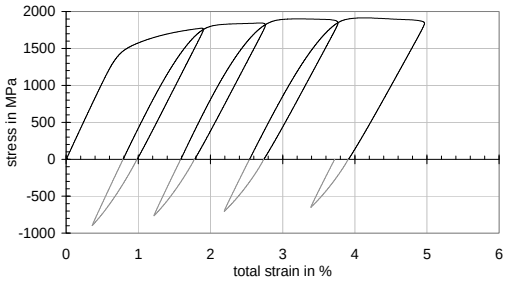

Figure 9 Stress-strain hystereses of the tension-compression test of condition E.

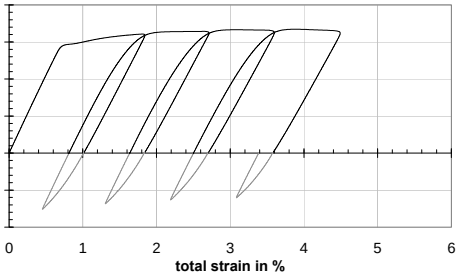

Figure 10 Stress-strain hystereses of the tension-compression test of condition F.

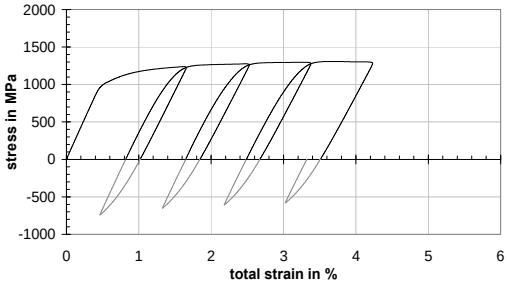

Figure 11 Stress-strain hystereses of the tension-compression test of condition G.

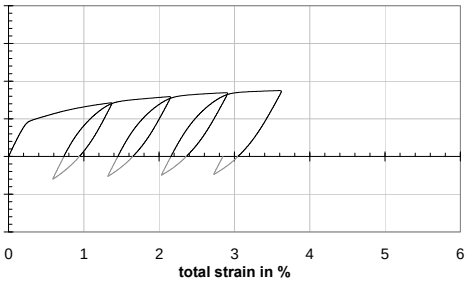

Figure 12 Stress-strain hystereses of the tension-compression test of condition H.

the fictitious stress at surface σ_R* was calculated by the applied bending momentum M_b and the axial section modulus W_b that depends on the specimen's geometry. The tests were carried out with a constant crosshead speed of 0.4mm/ min. The specimens were bent in one direction; thereafter they were unloaded and flipped by 180° for loading in the opposite direction.

2.3 Determination of Residual Stresses

The residual stress measurements in this work were carried out by X-ray stress determination in a ψ-diffractometer. CrKα radiation was used that penetrates steel according to [Engenmann et al. 1995] by about 5µm. To eliminate influences of machining, the specimens were electro polished by about 200µm. The $\sin^2\psi$ method [Eigenmann et al. 1995] with an elastic constant of ½ s_2=6.09*10^{-6} mm²/N was applied.

3. Experimental Results

3.1 Tension-Compression Tests

3.1.1 Stress-Strain Hystereses

The stress-strain hystereses of the four conditions E, F, G and H of 42CrMo4 are displayed in Figures 9-12.

Analogue to the tensile tests all material show different strengths and characteristic stress-strain behaviour. When unloading from σ_{max} all hystereses show a Young's modulus of about 210GPa first, like in forward loading. When unloading is continued, the curves deviate from linear-elastic behaviour and cause an increase of $\Delta\varepsilon_p$*. The normalized condition H (Figure 12) shows most non-linear unloading that can be detected easily. At reversed load one can see that there hardly is any yield stress anymore which means immediate plastic deformation. Since plastic deformations of about 0.2% were approached at reversed load in all heat treatment conditions, one can see that increasing plastic pre-strain leads to decreasing stress required for 0.2% plastic deformation at reversed load. In condition E the maximum stress reached at reversed load (0.2% proof stress) decreases from 900MPa at 1% plastic deformation to 650MPa at 4% plastic deformation, which is a decrease of about 30%. In the annealed martensite condition F the decrease is about 10%, in the bainite condition G about 25% and in the normalized condition H about 20%. The width of the hysteresis loop seems to be almost constant with increasing plastic deformation.

The stress-strain hysteresis of the normalized C45E is shown in Figure 13. Due to normalization the material is quite soft and offers only little strength.

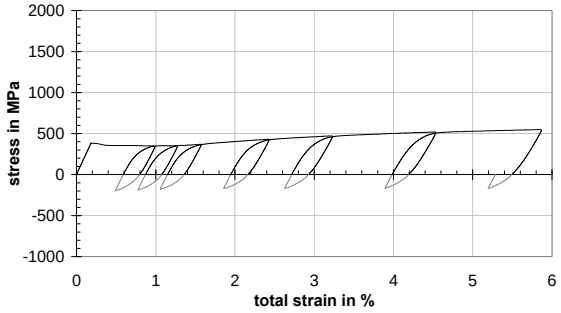

Figure 13 Stress-strain hystereses of the tension-compression test of C45E (condition N)

When reaching the plastic regime, the Lüders strain causes inhomogeneous elongation. Thereafter one can detect very little work hardening. The unloading procedure from pre-strain becomes more non-linear with increasing plastic deformation. The stress required for 0.2% plastic deformation at reversed load decreases form 200MPa to 160MPa which is about 20%.

3.1.2 Bauschinger Parameter

According to Figure 1, Bauschinger parameters were determined to characterize the quantity of the Bauschinger effect in the different heat treatment conditions.

Figure 14 shows the development of the related 0.1% proof stress after load reversal. All conditions show decreasing related yield strength with increasing plastic pre-strain. The smallest decrease of the related yield strength shows the bainite condition G; the normalized condition H shows an almost twice as large decrease. The annealed martensite condition E and F as well as the soft normalized C45E (condition N) can be found between these two extreme curves.

The non-linear unloading from forward deformation causes a plastic back deformation $\Delta\varepsilon_p^*$ that is illustrated in Figure 15. With increasing plastic pre-strain, the plastic back deformation increases in all conditions, the normalized condition H shows the largest plastic back deformation at all. Anyhow, $\Delta\varepsilon_p^*$ of C45E is even smaller than the one of condition G. Concerning 42CrMo4, at small plastic deformations nearly all conditions show similar values, but the bainite condition G increases slower than the martensite conditions F and E.

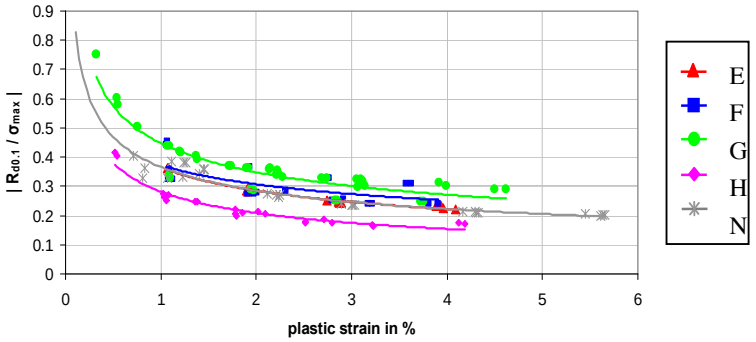

Figure 14 Related yield strength at reversed load of tension-compression test

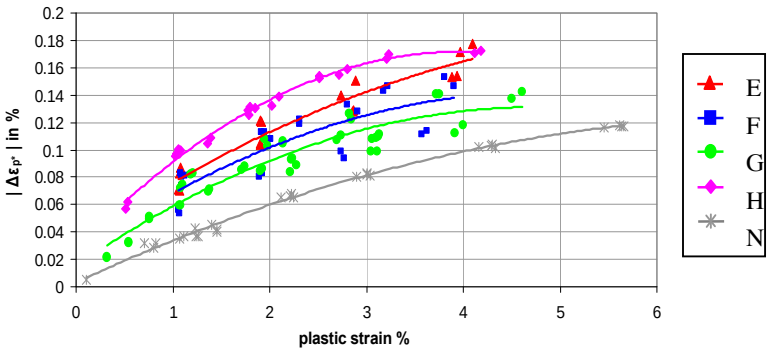

Figure 15 Plastic back-deformation $\Delta\varepsilon_p^*$ at unloading from pre-strain of tension-compression test.

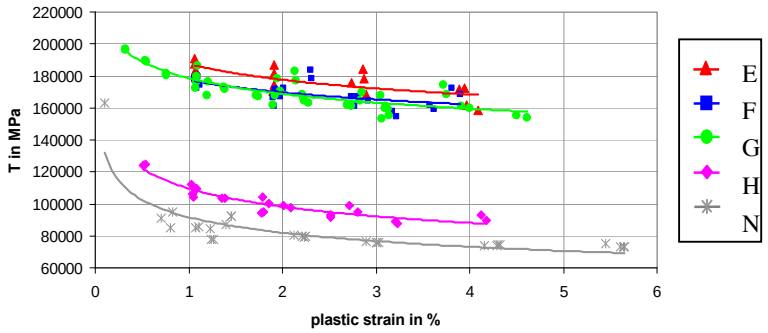

Figure 16 Tangent modulus T at reversed load of tension-compression test

Figure 16 shows the development of the tangent modulus T at reversed load in relation to plastic pre-strain. One can find that the tangent modulus decreases with increasing plastic pre-strain. When 3% plastic pre-strain is reached, the annealed martensite conditions E and F as well as the bainite condition G show a decrease of about 20%, based on a Young's modulus of 210GPa. The tangent modulus of condition H declines by about 50% and the one of condition N by about 60%.

5.2 Bending Tests

5.2.1 Stress-Strain Hystereses

Figures 17 to 20 show the stress-strain hystereses of the different states of 42CrMo4 at bending load.

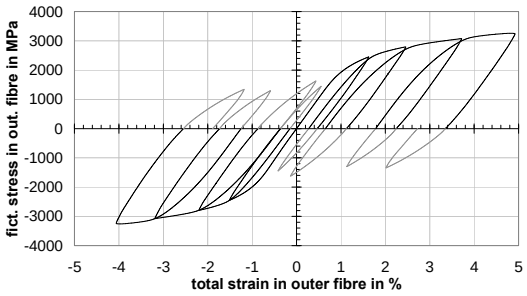

Figure 17 Stress-strain hystereses of the bending test of condition E

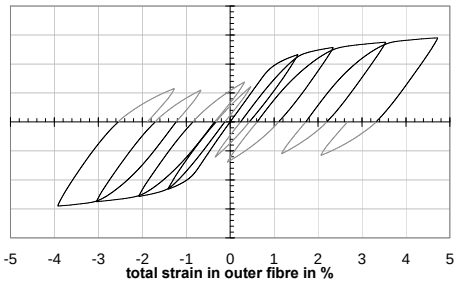

Figure 18 Stress-strain hystereses of the bending test of condition F

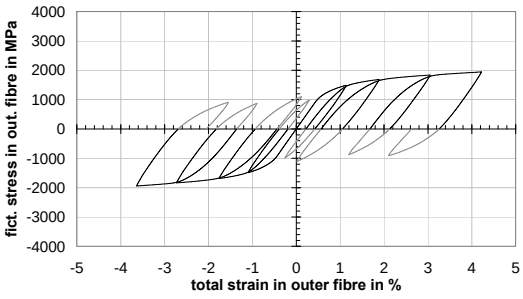

Figure 19 Stress-strain hystereses of the bending test of condition G.

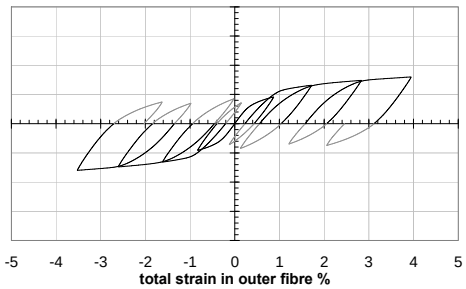

Figure 20 Stress-strain hystereses of the bending test of condition H

Tensile and compressive side of the specimen behave somewhat different since one can observe that the plastic strain is lower on the compressive side of the specimen, which could be an indicator for a strength-differential effect. The curves do not match in detail those of the tensile test since the fictitious stress in the outer fibre was applied. However, the largest work hardening occurs in the martensite condition E (Figure 17), the smallest in the normalized condition H (Figure 20), as it is the case in tensile tests. The unloading curve from pre-strain seems to be linear at the very beginning of unloading and becomes more non-linear when the load approaches to zero.

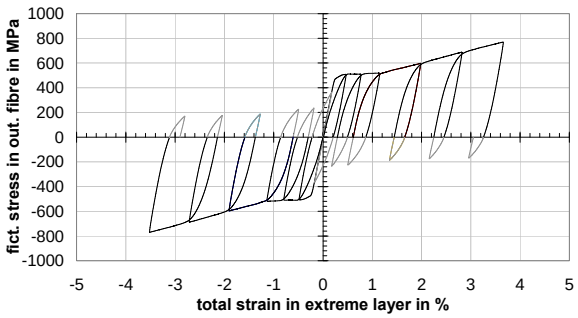

Figure 21 Stress-strain hystereses of the bending test of C45E (condition N)

In addition, the stress-strain hysteresis of C45E was investigated, see Figure 21. Like in the tensile test, the Lüders strain is clearly visible, followed by work hardening. The hysteresis loops are quite slim. Anyhow, the material has a much lower strength than 42CrMo4.

5.2.2 Bauschinger Parameter

The related yield strength, shown in Figure 22, expresses the development of the 0.1%-proof stress after load reversal. The effect of different strengths of the materials due to the heat treatments or work hardening is taken into account by the division of R by $\sigma_{max.}$ The diagram shows both the development of the tensile and the compressive side of the specimen.

One can see that plastic deformation causes decay in the related yield strength down to 10-20%. This means that the yield strength at load reversal decreased by about 80-90% if related to the maximum stress reached at pre-strain. The curves show that tensile and compressive side behave quite similarly.

According to the diagram one could guess that harder conditions have a somewhat larger decrease than softer conditions, but this observation does not count in general since e.g. condition E shows a smaller decrease than condition F.

Figure 23 demonstrates the plastic back deformation which is an indicator for the non-linear unloading behaviour. Increasing plastic pre-strain causes an increasing plastic back deformation during unloading from pre-strain. It is obvious that the tensile and the compressive side show a different behaviour which leads to asymmetric curves. In general one can say that there is no evidence that softer materials show a smaller back deformation at unloading since the soft condition H as well as the annealed martensite condition F shows similar values. Anyhow, all conditions seem to level off at about ±3 % plastic pre-strain.

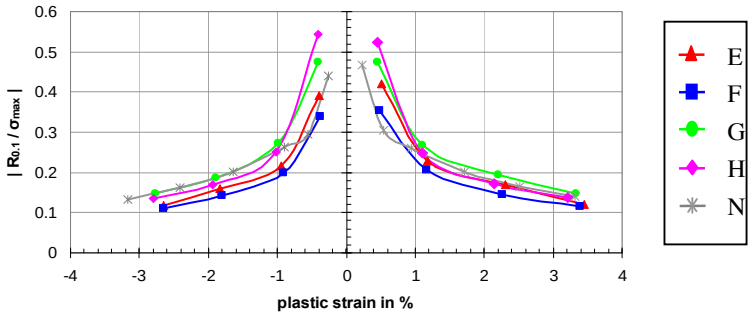

Figure 22 Related yield strength at reversed load of bending test

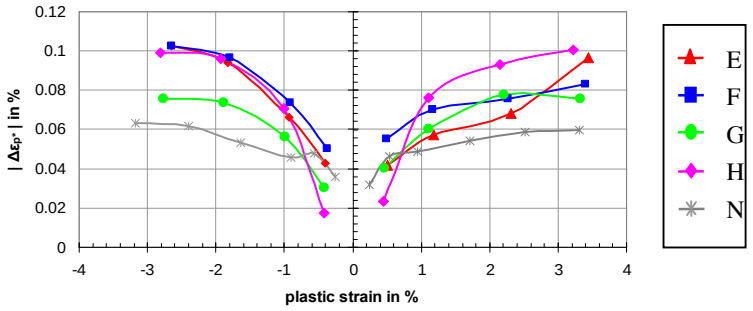

Figure 23 Plastic back deformation $\Delta\varepsilon_p$* at unloading from pre-strain of bending test

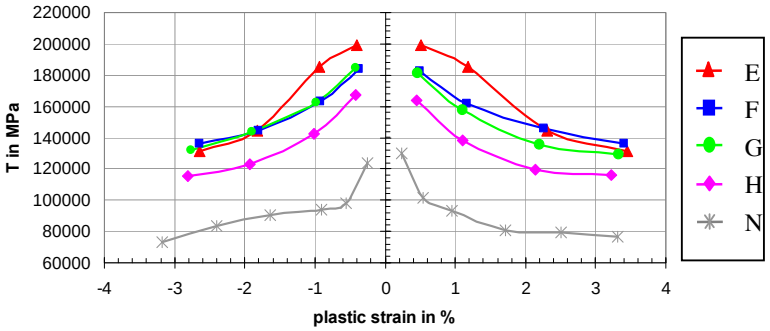

Figure 24 Tangent modulus at reversed load of bending test

Figure 24 illustrates the development of the tangent modulus T when load is reversed at different stages of plastic pre-strain. With increasing plastic pre-strain the tangent modulus T decreases. Based on a Young's modulus of 210GPa, the tangent modulus of the annealed martensite conditions E and F and the bainite condition G decrease by about 30% when 3% plastic strain are reached. The T-modulus of the normalized condition H decreases by about 50% and the one of condition N even by about 60%. The curves of tensile and compressive side are symmetric. According to Figure 24, one can assume that there is a correlation between hardness and the tangent modulus T at load reversal, since the softer the material, the smaller the tangent modulus.

3.2.3 Residual Stress Development at Bending

To measure the residual stresses on the tensile and the compressive side of specimen in dependency of the applied plastic deformation, the specimens were electrolytically polished and multiply loaded and unloaded. When the specimens were load-free, a residual stress measurement was carried out. When the deformation reached 2.5% plastic strain, the load was reversed and the specimens were loaded and unloaded in the opposite direction for several times.

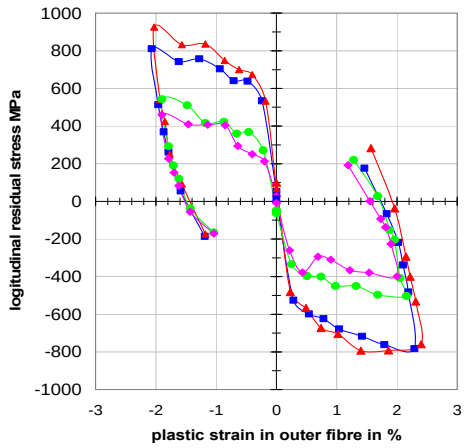

Figure 25 Residual stress development in outer layers during plastic deformation

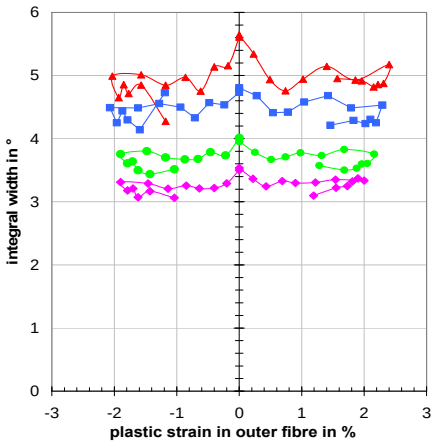

Figure 26 Integral width development in outer layers during plastic deformation

Figure 25 indicates that bending causes compressive residual stresses at the tensile side and tensile residual stresses at the compressive side of the specimen. In general one can see that the stronger the material the higher the developing residual stress in the material. At small plastic strains the residual stresses rise rapidly in the outer fibres first, but slow down at further deformation. When load is reversed, the residual stresses decrease rapidly and change their sign at only 0.5% back deformation. Furthermore it can be observed that the residual stress states are more diversified on the former tensile side than on the former compressive side after load is reversed. In addition to that one can see that the maximum surface strain is smaller at the compressive side than at the tensile side, which indicates a strength differential effect (SD- effect).

The integral width (IW) in Figure 26 represents the change in the inhomogeneous microstress during plastic deformation. At small plastic deformations the IW decreases by 10%. During further pre-strain the IW stays almost constant. When load is reversed one can detect another decrease in IW by about 3%.

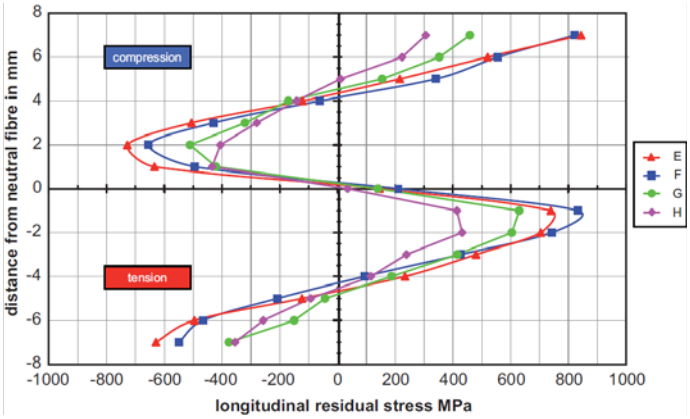

Figure 27 Residual stress development along bending height at 2% plastic pre-strain

3.2.4 Residual Stress Distribution along Bending Height

Plastic deformation of a bending specimen is accompanied by the development of an inhomogeneous stress state in the material, since on the one side the specimens is in tension and on the other one it is in compression. The neutral fibre has to be load-free.

The characteristic, triple zero-crossing residual stress distribution of a plastically deformed specimen can be observed in Figure 27. The residual stresses that develop are not symmetric to the neutral fibre: In the outer fibres of condition F, residual stresses of -550MPa at the tensile side and +850MPa on the compressive side occur. Close to the neutral fibre stresses of +850MPa on the tensile side and -650MPa on the compressive side are found. The residual stresses measured at the specimen's top and bottom side match the results of Figure 25 at about 2% plastic strain. Since the deformation is inhomogeneous there occur residual stresses close to the neutral fibre, which have about the same value than those in the outer fibre. Moreover, a direct relation between the residual stresses and the strength of the material can be found: The annealed martensite conditions E and F show somewhat higher residual stress than the bainite condition G or the normalized condition H.

3.2.5 Strength-Differential Effect (SD-Effect)

The SD-effect describes the phenomenon that specimens show different strengths under tensile or compressive load when strained to a certain plastic deformation. In the investigations published in this work, this phenomenon is expressed as "different strains at certain stress", since in case of bending the stress is a calculated value due to geometrical dimensions of the specimen assuming symmetric behaviour of tensile and compressive side.

The SD effect of bending specimens is shown exemplarily in Figure 28 for the high-strength condition E. By point reflection of the third sector one can easily compare tensile and compressive side. In addition, the difference between the strain of tensile and compressive side at the unloaded specimen was calculated for all conditions examined in this work. The result is shown in Figure 29.

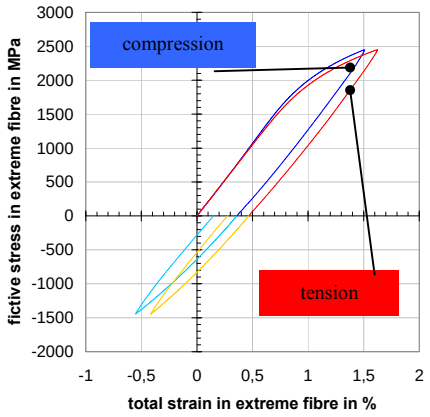

Figure 28 SD-effect in first tensile and compressive cycle of condition E

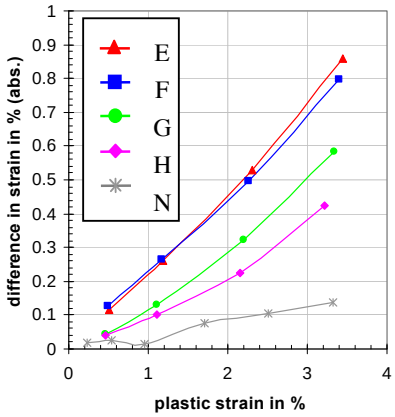

Figure 29 Strain differences between tensile and compressive side of bending specimen

One can see that the SD-effect is related to hardness and strength of the material. With increasing plastic deformation, the difference in strain on tensile and compressive side rises. The softer the material the smaller is the deviation between both sides.

4. Discussion

In the investigated heat treatment conditions of the steel 42CrMo4 a clear Bauschinger effect with its characteristic changes in the strain hardening curve can be observed. Especially when load is reversed there occur much lower yield strengths than if deformed further on in the direction of pre-strain. This effect even increases with higher plastic deformation in pre-strain. At high pre-strains, the Bauschinger effect seems to level off and reaches a certain limit, like it was examined in prior investigations [Abel et al. 1972].

The results found in this work show an obvious dependency of the magnitude of the Bauschinger effect on the heat treatment of the materials. One can observe the following tendencies: The bainite condition of 42CrMo4 shows the smallest decrease in the related yield strength and hereby the smallest Bauschinger effect. This behaviour occurs at homogeneous uniaxial load of tension-compression tests as well as in bending test with load reversal. By contrast, the largest Bauschinger effect can be observed for the ferrite/ pearlite condition of the steels. According to Figure 14, the hardened and low annealed conditions E and F can be found in-between the bainite and the ferrite condition. Comparing the low annealed steels only one can see that the one with the higher annealing temperature shows a Bauschinger effect that is somewhat larger. The reason could be the large amount of precipitated carbides for higher tempering temperatures. The ferrite/ pearlite conditions act as a two-phase material which enables the possibility developing larger back-stresses and causing an increase in the Bauschinger effect.

When comparing tension-compression tests and bending tests one can observe that the tendencies mentioned before are not consistent. At bending load the related yield strength shows even smaller values for the low annealed martensite conditions than for the ferrite/ pearlite conditions. So far it is not known if this is due to existing macro residual stresses in the material or due to application of the “fictitious stress” for characterization of bending load.

The occurrence of the plastic back strain $\Delta\varepsilon_p^*$ at bending (Figure 23) and tension-compression (Figure 15) show that unloading is linear elastic in no way. Hereby larger plastic back strains can be observed at the normalized condition H than at the annealed martensite and bainite conditions respectively. In contrast the normalized C45E shows the smallest plastic back strain in this work which does not give any evidence for a correlation between strength and the magnitude of the Bauschinger effect.

The kind of residual stresses development in the material plays a large role for the Bauschinger effect. Inhomogeneous deformation of a bending specimen causes plastic deformation in the outer fibres but only an elastic deformation in the core. This causes macro residual stresses when the specimen is unloaded. Superposition with micro residual stresses due to changes in microstructure leads to the characteristic residual stress state of plastically deformed bending specimens like shown in Figure 27. Over there the influence of strength on the development of residual stresses becomes visible. Along the bending height, residual stresses increase at surface as well as inside the specimen with increasing strength of the material. Since the tensile and the compressive side show different (absolute) values of residual stresses, further examination shall be done for finding the origin of this phenomenon.

The behaviour of the integral width of X-ray diffraction is quite peculiar. At small plastic deformations the examined conditions of 42CrMo4 show a decrease in integral width. Since plastic deformation typically causes increasing integral widths due to increasing inhomogeneous micro stresses, this indicates a rearrangement of dislocation arrangements for reaching energetically advantageous conditions. According to Abel [Abel et al. 1972], the decrease in integral width at reversed load is caused by the change in the dislocation arrangement.

So far, in this work the strength differential effect was systematically investigated at bending test specimens only. In every examined case in this work, the strain in the outer fibre is somewhat smaller at the compressive side than at the tensile side, but only the high-strength conditions are supposed to show a SD-effect. Softer conditions rather show a change in the cross sectional shape of the bending specimen that causes different stress and thereby different strain in the outer fibres of tensile and compressive side.

5. Conclusions

- A Bauschinger effect occurs in all studied conditions at reversed load.
- Two-phase materials seem to show a larger Bauschinger effect than single-phase like materials.
- Tension-compression and bending tests show different results concerning the Bauschinger effect. So far it is not clear if the reason is due to the use of “fictitious stress” or the influence of macro residual stresses.
- The existence of plastic back-deformation $\Delta\varepsilon_p^*$ indicates that unloading is a non-linear process in all cases.
- There is no evidence for correlation of the materials’ strength and the magnitude of the Bauschinger effect.
- Residual stresses increase with increasing strength of the material.

- Plastic deformation of a bending specimen causes tensile residual stress at the compressive side and compressive residual stress at the tensile side after unloading.
- Macro residual stresses due to bending cause a characteristic residual stress curve along the bending height with triple zero-crossing: High residual stresses close to neutral fibre have similar value than those in outer fibres.
- Integral width decreases at small plastic deformation and load reversal which means a change in the dislocation arrangement.
- Strength differential effect occurs in bending tests at high-strength materials but at softer ones it is supposed to be due to a change in the shape of the specimen's geometry.

6. Acknowledgement

The authors are grateful to the Deutsche Forschungsgemeinschaft DFG for financial support of this project.

References

Abel, A.; Muir, H.: 1972, The Bauschinger effect and discontinuous yielding, *Philosophical Magazine,* **26:2**, pp. 489-504

Bauschinger, J. : 1886, Über die Veränderung der Elasticitätsgrenze und der Festigkeit des Eisens und Stahls durch Strecken und Quetschen, durch Abkühlen und durch oftmals wiederholte Beanspruchung; *Mittheilungen aus dem Mechanisch-Technischem Laboratorium der K. Tech. Hochschule in München*, **15**

Eigenmann, B; Macherauch, E.:1995, Röntgenographische Spannungsanalyse, *Mat.-wiss. u. Werkstofftechn.* **26**, pp.148-160,

Gokyu, I.; Kishi, T.: 1970, On the Bauschingereffect of Polycrystals, Proceed. of the thirteenth Japan Congress on Materials Research – Metallic Materials, pp.125-128

Heeß, K.: 1997, Maß- und Formänderungen infolge Wärmebehandlung von Stählen, 3rd ed., *expert Verlag*, Renningen

Hoff, H.; Fischer, G.: 1958, Beobachtungen über den Bauschinger-Effekt an weichen und mittelharten Stählen, *Sonderabdruck „Eisen und Stahl"* **78,** 19 p.1313/20

Klein, D.; Thoben, K.-D., Nowag, L.: 2005, Using Indicators to Describe Distortion Along a Process Chain, in: *1st International Conference on Distortion Engineering* by Zoch, H.-W.; Lübben, T.; Bremen

Li, C.-C.; Flasck, J.D.; Yaker, J.A.; Leslie, W.C.: 1978, On Minimizing the Bauschingereffect in Steels by Dynamic Strain Aging, *Metallurgical Transactions A* **9A**, January, pp. 85-89

Noster, U.; Scholtes, B.: 2003, Bauschingereffekt und mechanische Zwillingsbildung der Magnesiumlegierung AZ31, *HTM – Journal of Heat Treatment and Materials* **58**, pp.322-327

Pfeiffer, I.; Weber H.: 1980, Einfluss des Richtens auf das mechanische Verhalten von Federlegierungen, *Z. Werkstofftechn*. **11**, pp.319-324

Ring, M; Dahl, W.: 1993, Bauschingereffect in high strength tensile bolts, *steel research* **64:10,** 10 pp.522-525.

Schmidt, W.; Heimann, W.: 1976, Einfluß einer Wärmebehandlung auf den Bauschinger-Effekt und das Kriechverhalten bei Raumtemperatur bei dem hochfesten austenitischen Stahl X 3 CrNiMoNbN 23 17 nach vorangegangenem Kaltrecken, *Arch. Eisenhüttenwes*. **47:12**

Scholtes, B; Vöhringer. O.: 1986, Untersuchungen zum Bauschingereffekt von Ck45 in unterschiedlichen Wärmebehandlungszuständen, *HTM - Härtereitechnische Mitteilungen* **41:5,** pp.347-354

Scholtes, B.; Vöhringer, O. Macherauch, M.: 1985, Die Auswirkungen des Bauschingereffekts auf das Verformungsverhalten von normalgeglühtem Stahl Ck45, *steel research* **56:3**, pp.157-162

Scholtes, B.: 1980, Die Auswirkungen des Bauschingereffekts auf das Verformungsverhalten technisch wichtiger Vielkristalle; Dr.-Ing. Diss.; *Universität Karlsruhe*, Germany

Scholtes, B., Vöhringer, O; Macherauch E.: 1983, Bauschingereffect and Buckling Behaviour of the Pressure Vessel Steel 20MnMoNi5 5, *Ferritic Steels in Nuclear Technologies*, ed. by J.W. Davies and D.J. Michel, AIME TMS STP, pp.45-50

Scholtes, B; Vöhringer, O.: 1986, Untersuchungen zum Bauschingereffekt an Kupfer und homogenen Kupferlegierungen, *Z. Metallkunde*, **77:9**, pp.595-602

Woolley, R. L.: 1953, The Bauschingereffect in some Face-centered and Body-centered Cubic Metals, *Phil. Mag.* **44**, pp.597-618